Pergamon International Journal of Machine Tools & Manufacture 40 (2000) 2175–2192

INTERNATIONAL JOURNAL OF
MACHINE TOOLS
& MANUFACTURE
DESIGN, RESEARCH AND APPLICATION

Modeling micro-end-milling operations. Part II: tool run-out

W.Y. Bao, I.N. Tansel *

Mechanical Engineering Department, Florida International University, Center for Engineering and Applied Sciences, 10555 West Flagler Street, Miami, FL 33174, USA

Received 28 February 2000; received in revised form 9 June 2000; accepted 15 June 2000

Abstract

The effect of run-out is clearly noticed in micro-end-milling operations, while the same run-out creates negligible change at the cutting force profile of conventional end-milling operations. In this paper, the cutting force characteristics of micro-end-milling operations with tool run-out are investigated. An analytical cutting force model is developed for micro-end-milling operations with tool run-out. The proposed model has a compact set of expressions to be able to estimate the cutting force characteristics very quickly compared to the numerical approaches. The cutting forces of micro-end-milling operations simulated by the proposed model had good agreement with the experimental data. © 2000 Elsevier Science Ltd. All rights reserved.

Keywords: Manufacture; Micro-tools; End-milling; Modeling

1. Introduction

Tool run-out mainly depends on the characteristics of the spindle and tool holder. A small run-out that affects the cutting force profile of conventional end-milling operations (CEMO) very little creates drastic force variations in micro-end-milling operations (MEMO) [1]. In MEMO, the tool run-out to tool diameter (r_o/r) ratio becomes very big compared to CEMO. It is very common to see that only one cutting edge of a two-flute micro-end-mill performs the machining operations alone while the other edge doesn't touch the workpiece at all. When one of the cutting edges starts to perform all or most of the cutting operations, the force variation increases significantly. The tool wears out much more quickly, and the probability of tool breakage increases.

To select the optimal cutting condition of MEMO, it is very helpful to be able to estimate the cutting force characteristics in a wide cutting parameter range if the tool run-out is known. To

* Corresponding author. Tel.: +1-305-348-1932; fax: +1-305-348-3304.
E-mail address: tanseli@eng.fiu.edu (I.N. Tansel).

PII: S0890-6955(00)00055-9

Nomenclature

x	feed direction coordinate
y	normal direction coordinate
z_c	the coordinate perpendicular to the x–y plane
t	time (s)
F_t	tangential cutting force (N)
F_r	radial cutting force (N)
F_x	feed direction cutting force (N)
F_y	normal direction cutting force (N)
r	tool radius (inch)
Z	the number of tool teeth
z	the ordinal number of tool teeth
β	tooth helix angle (rad)
n	spindle speed (rpm)
ω	spindle circle speed (1/s)
f	feed rate (ipm)
f_t	feed per tooth (inch)
a	depth of cut (inch)
b	width of cut (inch)
θ	tool cutting angle (rad)
θ_s	integrating start angle (rad)
θ_e	integrating end angle (rad)
h	chip thickness (inch)
λ	leading angle (rad)
α	engagement angle (rad)
φ	workpiece cutting angle (rad)
ψ	tool cutter angle (rad)
F_u	unit force (N)
p	proportional factor
K_m	material coefficient (N/cm^2)
r_o	run-out length (inch)
γ	run-out angle (rad)

consider the tool run-out, the chip thickness expression [2] was modified [3]. Development of a model in frequency domain was considered [4]. The computer-based numerical model was introduced [5]. Various models and numerical procedures have been developed [6–10] to estimate the cutting forces for CEMO. However, none of them offers a compact expression to calculate the cutting forces for MEMO with tool run-out. In this paper, the analytical model of MEMO [1] was improved further by considering tool run-out. The cutting force expressions were simplified by eliminating the insignificant components of the chip thickness expression to obtain the results in a more compact form. The proposed model can be used very conveniently to study the cutting

force characteristics, to estimate the tool run-out, to select the optimal cutting conditions, to monitor the operating conditions, and to estimate the surface quality.

In the following sections, a new model for MEMO with tool run-out will be introduced. The proposed model will be compared to the conventional approaches and MEMO without tool run-out. The validity of the proposed model is evaluated by comparing the simulated and experimental cutting force profiles.

2. Cutting force modeling of micro-end-milling operations with tool run-out

Considering the tool tip trajectory and chip thickness, an analytical cutting force model was derived for MEMO without tool run-out [1]. For MEMO with tool run-out, the trajectory of the tool tip can be written with the following equations (Fig. 1):

$$x=\frac{ft}{60}+r\sin\left(\omega t-\frac{2\pi z}{Z}\right)+r_o\sin(\omega_t+\gamma) \tag{1}$$

$$y=r\cos\left(\omega t-\frac{2\pi z}{Z}\right)+r_o\cos(\omega t+\gamma) \tag{2}$$

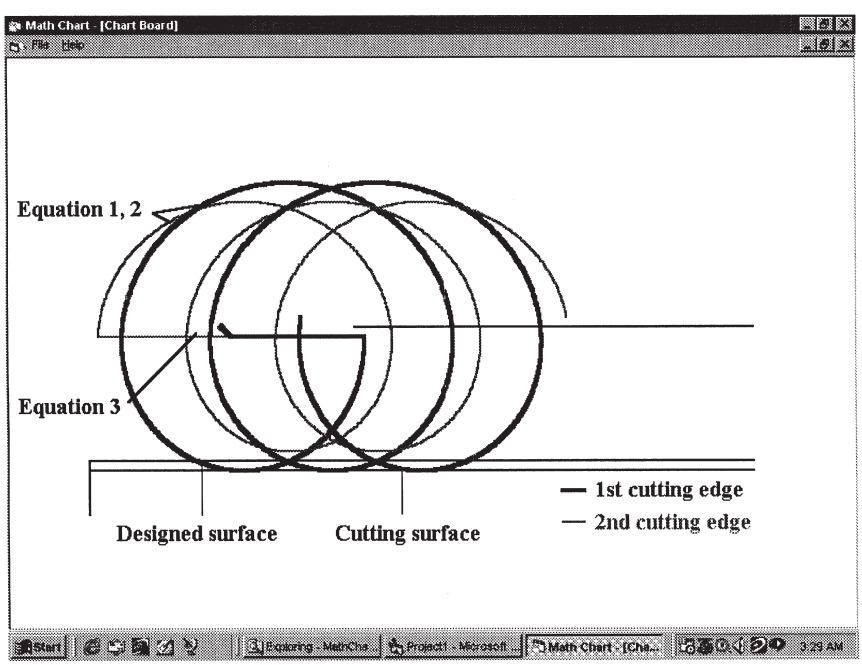

Fig. 1. Trajectory of the two-flute tool tip of micro-end-milling operations with a 45° tool run-out angle.

The trajectory of tool cutting edges can be written as:

$$\left[x-\left(\frac{ft}{60}+r_o\frac{\sin\gamma}{\cos\omega t}\right)\right]\cos\left(\omega t-\frac{2\pi z}{Z}\right)-y\sin\left(\omega t-\frac{2\pi z}{Z}\right)=0 \tag{3}$$

where: $\omega=\dfrac{2\pi n}{60}$

$Z=2$ and $z=0$, 1 for two−flute tools

$Z=4$ and $z=0$, 1, 2, 3 for four−flute tools

The intersection of the first cutting edge tip at time t_0 with angle θ_0 and the second cutting edge at time t_1 with angle θ_1 can be solved from Eqs. (1)–(3).

$$\left[\frac{f}{60\omega}(\omega t_0-\omega t_1)-r_o\frac{\sin\gamma}{\cos\omega t_1}\right]\cos\left(\omega t_1-\frac{2\pi(z+1)}{Z}\right)+r\sin\left(\omega t_0-\omega t_1+\frac{2\pi}{Z}\right)+r_o\sin\left(\omega t_0-\omega t_1+\gamma+\frac{2\pi(z+1)}{Z}\right)=0$$

Considering geometric conditions, it can be simplified as:

$$\left\{\frac{f}{2\pi n}\left(\frac{2\pi}{Z}-\delta\right)+r_o\frac{\sin\gamma}{\cos\left[\dfrac{\pi}{2}-\theta_1+\dfrac{2\pi(z+1)}{Z}\right]}\right\}\cos\left(\frac{\pi}{2}-\theta_1\right)=r\sin\delta+r_o\sin\left(\delta+\gamma+\frac{2\pi z}{Z}\right)$$

where: $\theta_z=\left(1+\dfrac{4z}{Z}\right)\dfrac{\pi}{2}-\omega t_z$

$\delta=\theta_{z+1}-\theta_z$

$\omega t_{z+1}-\omega t_z=\dfrac{2\pi}{Z}-\delta$

From the above equation, the computing angle δ can be solved.

$$\delta\approx\frac{f_t\dfrac{\cos\theta}{r}+\dfrac{r_o}{r}\dfrac{\sin\gamma\cos\theta}{\cos\left[\theta+\dfrac{2\pi(z+1)}{Z}\right]}-\dfrac{r_o}{r}\sin\left(\gamma+\dfrac{2\pi z}{Z}\right)}{1+f_t\dfrac{Z\cos\theta}{2\pi r}+\dfrac{r_o}{r}\cos\left(\gamma+\dfrac{2\pi z}{Z}\right)}$$

where: $f_t=\dfrac{f}{nZ}$

$$\theta=\frac{\pi}{2}-\theta_1$$

Let's consider the two-flute end-mill case. The computing angle δ can be simplified.

$$\delta\approx\frac{f_t\dfrac{\cos\theta}{r}-(-1)^z 2\dfrac{r_o}{r}\sin\gamma}{1+f_t\dfrac{\cos\theta}{\pi r}+(-1)^z\dfrac{r_o}{r}\cos\gamma}$$

where: z=0, 1

The computing feed rate is defined as:

$$f_c=\frac{f}{60}(t_1-t_0)+r_o\sin\gamma\left(\frac{1}{\cos\omega t_1}-\frac{1}{\cos\omega t_0}\right)$$

Considering geometric conditions and assuming $\theta_0\approx\theta_1=\theta$ (because δ is small), it can be rewritten as:

$$f_c=\frac{f}{2\pi n}(\pi-\delta)-(-1)^z 2r_o\frac{\sin\gamma}{\cos\theta}$$

Substituting the computing angle δ, it becomes:

$$f_c\approx f_t[1+(-1)^z\frac{2r_o}{\pi r}\sin\gamma]-f_t^2\frac{\cos\theta}{\pi r}-(-1)^z 2r_o\frac{\sin\gamma}{\cos\theta}$$

Also considering geometry and assuming $\Delta r_0\approx\Delta r_1=\Delta r$, there is:

$$[r+(-1)^z\Delta r]^2=H^2+f_c^2-2Hf_c\cos(\pi-\theta_1)$$

The non-cutting edge length H can be solved from the above equation.

$$H=-f_c\sin\theta+\sqrt{[r+(-1)^z\Delta r]^2-(f_c\cos\theta)^2}$$

The chip thickness is:

$$h=[r-(-1)^z\Delta r]-H=[r-(-1)^z\Delta r]+f_c\sin\theta-\sqrt{[r+(-1)^z\Delta r]^2-(f_c\cos\theta)^2}$$

Substituting the computing feed rate f_c to the above expression and simplifying it, the chip thickness becomes:

$$h \approx f_t[1+(-1)^z \frac{2r_o}{\pi r}\sin\gamma)]\sin\theta - \frac{1}{\pi r} f_t^2 \sin\theta\cos\theta + \frac{1}{2r} f_t^2 \cos^2\theta - (-1)^z 2r_o \cos\gamma \tag{4}$$

The tool run-out is presented in the first and fourth items of the expression Eq. (4). The fourth term of expression Eq. (4) is a major contributor to the run-out. It reaches a maximum value when the run-out is parallel to the tool cutting edges (γ=0°), and turns to a minimum value when the run-out is perpendicular to the tool cutting edges (γ=90°). The second part of the first term of expression Eq. (4) is an additional run-out. When γ=90°, the tool run-out reduces to the minimum level and almost disappears. It can be neglected in most CEMO because of $r_o/r \ll 1$. For two-flute end-mills, if $2r_o \cos\gamma$ is larger than f_t, only one cutting edge performs the machining operations. In expression Eq. (4), the z parameter presents the different chip thickness of each cutting edge.

The cutting force can be derived by the following expressions.

$$dF_x = -2F_u\left[\left(1+(-1)^z\frac{2r_o}{\pi r}\sin\gamma\right)\sin\theta - \frac{1}{\pi r} f_t \sin\theta\cos\theta + \frac{1}{2r} f_t \cos^2\theta - (-1)^z 2\frac{r_o}{f_t}\cos\gamma\right](\cos\theta\, d\theta + p\sin\theta\, d\theta)$$

$$dF_y = 2F_u\left[\left(1+(-1)^z\frac{2r_o}{\pi r}\sin\gamma\right)\sin\theta - \frac{1}{\pi r} f_t \sin\theta\cos\theta + \frac{1}{2r} f_t \cos^2\theta - (-1)^z 2\frac{r_o}{f_t}\cos\gamma\right](\sin\theta\, d\theta - p\cos\theta\, d\theta)$$

After integration, the cutting force expressions are:

$$F_x = F_u\left[C_3\frac{f_t}{r}\sin^3\theta + C_4\frac{f_t}{r}\cos^3\theta - (1+C_5)\sin^2\theta + \frac{1}{2}p(1+C_5)\sin 2\theta + \left(C_6 - \frac{f_t}{r}\right)\sin\theta - pC_6\cos\theta - p(1+C_5)\theta\right]\Bigg|_{\theta_s}^{\theta_e} \tag{5}$$

$$F_y = F_u\left[C_4\frac{f_t}{r}\sin^3\theta - C_3\frac{f_t}{r}\cos^3\theta - p(1+C_5)\sin^2\theta - \frac{1}{2}(1+C_5)\sin 2\theta + p\left(C_6 - \frac{f_t}{r}\right)\sin\theta + C_6\cos\theta + (1+C_5)\theta\right]\Bigg|_{\theta_s}^{\theta_e} \tag{6}$$

where:

$$F_u = \frac{K_m r f_t}{2 \tan \beta}$$

$$C_3 = \frac{1}{3}\left(1 + p\frac{2}{\pi}\right)$$

$$C_4 = \frac{1}{3}\left(p - \frac{2}{\pi}\right)$$

$C_5 = \pm\frac{2r_o}{\pi r}\sin\gamma$, ± for both cutting edges, respectively

$C_6 = \pm\frac{4r_o}{f_t}\cos\gamma$, ± for both cutting edges, respectively

According to the experimental data, the proportional factor is usually selected as 0.3.

To calculate the cutting force by using the model, the four computational parameters are introduced.

- Tool cutter angle ψ is defined as:

$$\Psi = 2\pi/Z$$

- Workpiece cutting angle φ is defined as:

$$\varphi = \arccos[(r-a)/r]$$

- Engagement angle α is defined as:

$$\alpha = b \tan \beta / r$$

- The leading angle λ can be derived from expression Eq. (11) by considering θ=0°.

$$\sin\lambda = \frac{2r_o \cos\gamma - \frac{1}{2r} f_t^2 \cos^2\lambda}{f_t\left(1 + \frac{2r_o}{\pi r}\sin\gamma\right) - \frac{1}{\pi r} f_t^2 \cos\lambda}$$

If $f_t/r \ll 1$ and $r_o/r \ll 1$, it becomes:

$$\lambda = \arcsin\left(\frac{2r_o}{f_t}\cos\gamma\right)$$

Most of MEMO can be considered in the following three cases.

2.0.1. Case 1

$\alpha \le \varphi+\lambda$ and $\alpha+\varphi+\lambda \le \psi$

In up-milling operations

section 1:	$[-\lambda,\ \alpha-\lambda]$	$\theta_s=-\lambda$	$\theta_e=\theta$
section 2:	$[\alpha-\lambda,\ \varphi]$	$\theta_s=\theta-\alpha$	$\theta_e=\theta$
section 3:	$[\varphi,\ \varphi+\alpha]$	$\theta_s=\theta-\alpha$	$\theta_e=\varphi$

In down-milling operations

section 1:	$[\pi-\varphi,\ \pi-\varphi+\alpha]$	$\theta_s=\pi-\varphi$	$\theta_e=\theta$
section 2:	$[\pi-\varphi+\alpha,\ \pi+\lambda]$	$\theta s=\theta-\alpha$	$\theta_e=\theta$
section 3:	$[\pi+\lambda,\ \pi+\lambda+\alpha]$	$\theta_s=\theta-\alpha$	$\theta_e=\pi+\lambda$

2.0.2. Case 2

$\alpha \ge \varphi+\lambda$ and $\alpha+\varphi+\lambda \le \psi$

In up-milling operations

section 1:	$[-\lambda,\ \varphi]$	$\theta_s=-\lambda$	$\theta_e=\theta$
section 2:	$[\varphi,\ \alpha-\lambda]$	$\theta_s=-\lambda$	$\theta_e=\varphi$
section 3:	$[\alpha-\lambda,\ \varphi+\alpha]$	$\theta_s=\theta-\alpha$	$\theta_e=\varphi$

In down-milling operations

section 1:	$[\pi-\varphi,\ \pi+\lambda]$	$\theta_s=\pi-\varphi$	$\theta_e=\theta$
section 2:	$[\pi+\lambda,\ \pi-\varphi+\alpha]$	$\theta_s=\pi-\varphi$	$\theta_e=\pi+\lambda$
section 3:	$[\pi-\varphi+\alpha,\ \pi+\lambda+\alpha]$	$\theta_s=\theta-\alpha$	$\theta_e=\pi+\lambda$

2.0.3. Case 3

$\alpha+\varphi+\lambda \ge \psi$

Because of overlap, the cutting force of the overlapped part is equal to the sum of the cutting forces of both cutting edges.

3. Experimental setup

The experiments of MEMO were performed in the Mechatronics Lab of the Mechanical Engineering Department of Florida International University and the Engineering Prototype Center of the Radio Technology Division of Motorola Inc. Three different types of milling machines were used in the experiments. The test workpiece was set on a Kistler 9257B 3-component piezoelectric dynamometer that was installed on the table of the machine tool. Two components of the cutting force were collected by using Nicolet 310 and Nicolet integra model 10 digital oscilloscopes through a Kistler 3-channel charge amplifier. The typical experimental setup, equipment and cutting conditions are presented [1].

4. Results and discussion

In this section, the accuracy of the simulated cutting force profile of the proposed model is evaluated. The proposed model is compared with the conventional model and MEMO without the tool run-out model. The characteristics of the cutting force and tool run-out are discussed.

4.1. Typical tool run-out in micro-end-milling applications

In this study, tool run-out of MEMO was investigated experimentally by using two different types of tool holder. One of them was the conventional holder with a setscrew and the other used a collet to hold the tool. The tool run-out was calculated from the experimental cutting force data by using a run-out estimation program developed from the proposed model. This approach allowed the estimation of run-out at the tool tip. Even the wear-related shortening of the cutting edge was possible to detect by using the proposed model.

The results of two sets of experiments are presented in Table 1 and Table 2. In the first set of experiments, a two-flute 1/16″-diameter carbide end-mill was attached to a collet and an aluminum workpiece was cut at different conditions in a series of experiments. The test conditions included 15,000, 32,000 and 50,000 rpm spindle speed, 0.0005, 0.00075 and 0.001 ipm feed rate. Down-milling was performed with 0.020″ width of cut and 1/32″ depth of cut.

In the other set of experiments, a two-flute 1/16″-diameter high-speed steel (HSS) end-mill was attached to a conventional holder to machine an EDM POCO-3 graphite workpiece. The spindle speed was 15,000 rpm in the experiments. 30, 65 and 100 ipm feed rate, 1/16″, 0.100″ and 0.150″

Table 1
Experimental results of tool run-out with a collet holder

	Feed direction run-out			Normal direction run-out		
	Spindle speed (rpm)					
Feed rate (ipm)	15,000	32,000	50,000	15,000	32,000	50,000
0.00100	48%	10%	20%	9%	9%	24%
0.00075	50%	65%	47%	8%	9%	49%
0.00050	63%	55%	23%	0	0	35%

Table 2
Experimental results of tool run-out with a conventional holder

	Feed direction run-out			Normal direction run-out		
	Feed rate (ipm)					
Width of cut (inch)	30	65	100	30	65	100
0.1500	87%	87%	46%	72%	85%	71%
0.1000	40%	48%	63%	57%	54%	64%
0.0625	78%	86%	79%	56%	83%	60%

width of cut were tested. In all the machining operations, 50% overlapped (1/32″ depth of cut) down-milling was performed.

According to the test results, the holder with a collet had 0% to 65% run-out in different experiments. The average run-out was around 30%. The run-outs of the conventional holder were between 40% and 87%. The average was around 68%. The holder with a collet had much smaller run-out compared to the conventional holder. Usually smaller run-out means better surface quality, longer tool life and lower tool breakage probability in practical MEMO.

4.2. Verification of the proposed cutting force model

The proposed analytical model used ten parameters and one coefficient to represent the cutting forces of MEMO and CEMO without or with tool run-out.

- Three working condition variables: spindle speed (n), feed rate (f) and width of cut (b).
- Two tool run-out variables: run-out (r_o) and its angle (γ).
- Two cutting condition variables: tool cutting entry and exit angle, which presents depth of cut (a), and up- and down-milling.
- Three tool geometry variables: tool diameter ($2r$), helix angle (β) and the numbers of tool flutes (N).
- Material coefficient (K_m) is related to the tool and workpiece materials, which could be determined by a few experiments.

The proposed analytical cutting force model of MEMO with tool run-out can be presented as the following expressions:

$$F_x = F_u\left[C_3\frac{f_t}{r}\sin^3\theta + C_4\frac{f_t}{r}\cos^3\theta - (1+C_5)\sin^2\theta + \frac{1}{2}p(1+C_5)\sin 2\theta + \left(C_6 - \frac{f_t}{r}\right)\sin\theta - pC_6\cos\theta - p(1+C_5)\theta\right]\Bigg|_{\theta_s}^{\theta_e}$$

$$F_y = F_u\left[C_4\frac{f_t}{r}\sin^3\theta - C_3\frac{f_t}{r}\cos^3\theta - p(1+C_5)\sin^2\theta - \frac{1}{2}(1+C_5)\sin 2\theta + p\left(C_6 - \frac{f_t}{r}\right)\sin\theta + C_6\cos\theta + (1\right.$$

$$+C_5)\theta\Big]\Big|_{\theta_s}^{\theta_e}$$

If r_o=0, the model becomes the following form for MEMO without tool run-out [1].

$$F_x=F_u\left[C_1\frac{f_t}{r}\sin^3\theta+C_2\frac{f_t}{r}\cos^3\theta-\sin^2\theta+\frac{1}{2}p\sin 2\theta-\frac{f_t}{r}\sin\theta-p\theta\right]\Big|_{\theta_e}^{\theta_s} \tag{7}$$

$$F_y=F_u\left[C_2\frac{f_t}{r}\sin^3\theta-C_1\frac{f_t}{r}\cos^3\theta-p\sin^2\theta-\frac{1}{2}\sin 2\theta-p\frac{f_t}{r}\sin\theta+\theta\right]\Big|_{\theta_s}^{\theta_e}$$

If $f_t/r\ll 1$, the model becomes the following form for CEMO with tool run-out.

$$F_x=F_u\left[-\sin^2\theta+\frac{1}{2}p\sin 2\theta\pm\frac{4r_o}{f_t}\cos\gamma(\sin\theta-p\cos\theta)-p\theta\right]\Big|_{\theta_s}^{\theta_e} \tag{9}$$

$$F_y=F_u\left[-p\sin^2\theta-\frac{1}{2}\sin 2\theta\pm\frac{4r_o}{f_t}\cos\gamma(p\sin\theta+\cos\theta)+\theta\right]\Big|_{\theta_s}^{\theta_e} \tag{10}$$

If $f_t/r\ll 1$ and r_o=0, the model becomes the following form for CEMO without tool run-out. It has the exact same form as Tlusty and Macneil's model [2].

$$F_x=F_u\left[-\sin^2\theta+\frac{1}{2}p\sin 2\theta-p\theta\right]\Big|_{\theta_s}^{\theta_e} \tag{11}$$

$$F_y=F_u\left[-p\sin^2\theta-\frac{1}{2}\sin 2\theta+\theta\right]\Big|_{\theta_s}^{\theta_e} \tag{12}$$

That is said so that MEMO without the tool run-out model and Tlusty and Macneil's model are included in the proposed model.

The proposed cutting force model has been tested on the experimental data of hundreds of MEMO cases and very good agreement has been observed between the theoretical and experimental results. The results are presented in Table 3. The average error of maximum cutting force between the simulation by using the proposed model and experimental data is around 21%.

Table 3
Error between computational and experimental maximum cutting forces

Test no.	End-mill (two-flute)	Workpiece material	Spindle speed (rpm)	Feed rate (ipm)	Width of cut (inch)	Depth of cut (inch)	Error of cutting force between the simulation and test
1	1/16″ HSS	EDM POCO-3 graphite	15,000	30	0.1	1/32	28.0%
2	1/16″ HSS	EDM POCO-3 graphite	15,000	65	1/16	1/32	11.5%
3	1/16″ HSS	EDM POCO-3 graphite	15,000	65	0.1	1/32	17.2%
4	1/16″ HSS	EDM POCO-3 graphite	15,000	100	1/16	1/32	2.5%
5	1/16″ HSS	EDM POCO-3 graphite	15,000	100	0.1	1/32	12.7%
6	0.02″ HSS	EDM POCO-3 graphite	15,000	20	0.03	0.01	53.9%
7	0.02″ HSS	EDM POCO-3 graphite	15,000	70	0.01	0.01	26.1%
8	0.02″ HSS	EDM POCO-3 graphite	15,000	70	0.03	0.01	19.6%
9	0.02″ HSS	EDM POCO-3 graphite	15,000	70	0.05	0.01	0.0%
10	0.02″ HSS	EDM POCO-3 graphite	15,000	120	0.01	0.01	37.0%
Ave.							20.9%

The simulated and experimental feed and normal direction cutting force profiles are presented in Fig. 2 and Fig. 3. In the test, a two-flute 1/16″-diameter HSS end-mill cut was performed on an EDM POCO-3 graphite workpiece. Down-milling operations were performed with the cutting conditions of 15,000 rpm spindle speed, 100 ipm feed rate, 1/16″ width of cut and 1/32″ depth of cut. The tool run-out was 0.001″ with a 50-degree angle.

4.3. Model-based tool run-out and cutting force characteristics study

The maximum cutting force chart is a very useful tool to help operators in selecting the operating conditions. It can be easily calculated by using the proposed model instead of performing many tests. A model-based feed direction maximum cutting force chart is presented in Fig. 4. It had good agreement with the experimental one created by using a neural networks software (Fig. 5). The software called NNTool (Neural Networks Research Tool) was developed in 1995 and modified in 1996 [11]. In the presented case, a two-flute HSS end-mill with 0.020″-diameter machined an EDM POCO-3 graphite workpiece in down-milling operations. The work-

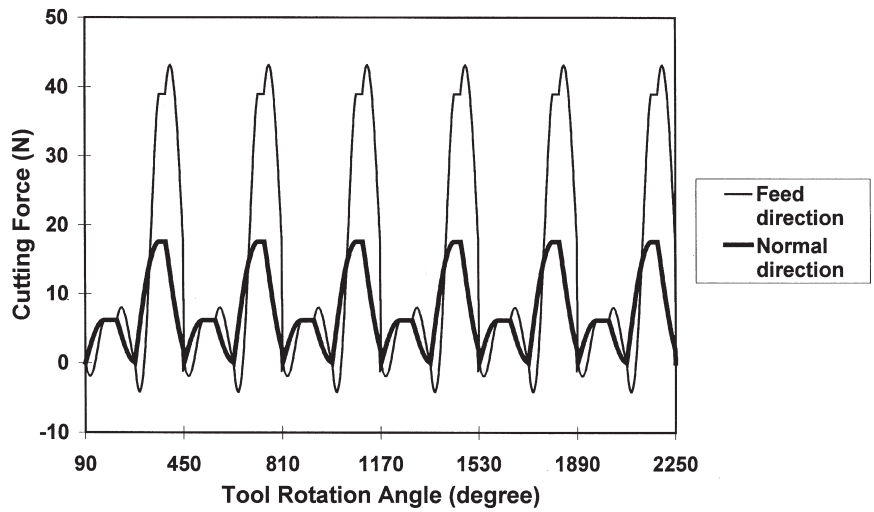

Fig. 2. Simulated cutting force profiles of micro-end-milling operations with tool run-out.

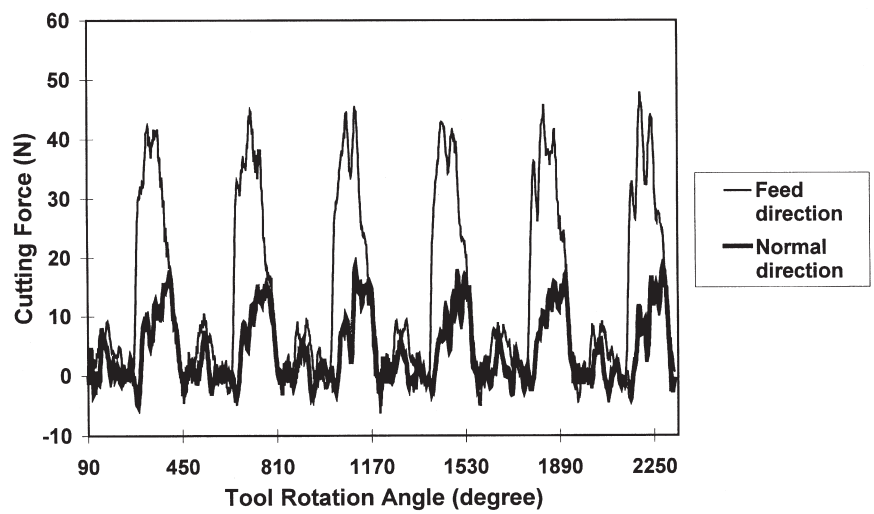

Fig. 3. Experimental cutting force signals of micro-end-milling operations with tool run-out.

ing conditions were 15,000 rpm spindle speed, 20 ipm to 120 ipm feed rate, 0.010″ to 0.050″ width of cut and 0.010″ depth of cut.

Tool holders with a setscrew are widely used in MEMO. When the setscrew is tightened, it pushes the tool towards one side and a small run-out is created. The line, called the offset line in this paper, between the ideal and actual centers of the tool is perpendicular to the setscrew. The offset depends on the tool holder design and tool installation. However, operators can adjust the angle between the offset line and the tool cutting edges while they install the tool. Based on the proposed approach, the relationship between this angle and the characteristics of the cutting force have been studied for two- and four-flute micro-end-mills.

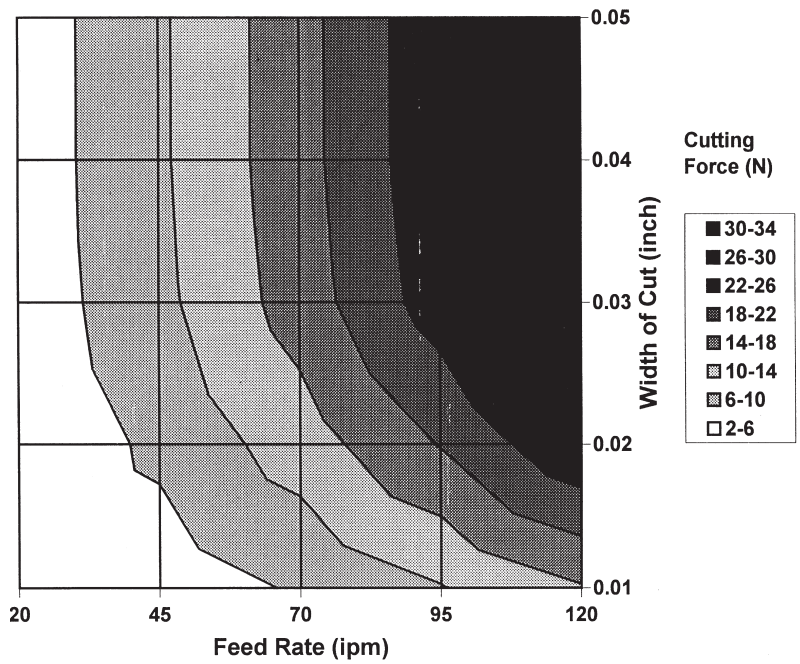

Fig. 4. Simulated feed direction maximum cutting force chart of micro-end-milling operations.

The variation of the normal direction maximum cutting force with different tool run-out was obtained by using a simulation program based on the proposed model and is presented in Fig. 6 and Fig. 7. The main indicator of the run-out is the difference between the cutting force lumps created by the tool cutting edges. These lumps are identical when the tool has no run-out. The difference between the lumps of the cutting edges increases with the run-out. It is possible to estimate the tool run-out by inspecting the lumps from the experimental cutting force data.

According to the simulations of MEMO with tool run-out, the cutting force variation of a two-flute end-mill reaches to its maximum when the offset line is parallel to the tool cutting edge (γ=0°, Fig. 8). The cutting force variation of a two-flute end-mill decreases to its minimum if the offset line is perpendicular to the cutting edge (γ=90°, Fig. 9). For a four-flute end-mill, the cutting force variation reaches to a maximum value when the offset line is parallel to the tool cutting edge (γ=0°). The cutting force variation shrinks to its smallest level when the offset line has a 45° angle with any two adjoining cutting edges (γ=45°, Fig. 10).

To minimize the cutting force variation, the tool should be carefully installed into the tool holder. The operator should adjust the offset line to be perpendicular to the cutting edges of the two-flute tools. For four-flute tools, the angle between the offset line and one of the cutting edges should be 45°.

5. Conclusion

A new compact analytical cutting force model was developed for MEMO with tool run-out. The model is capable of simulating the cutting force profiles of MEMO and of estimating the

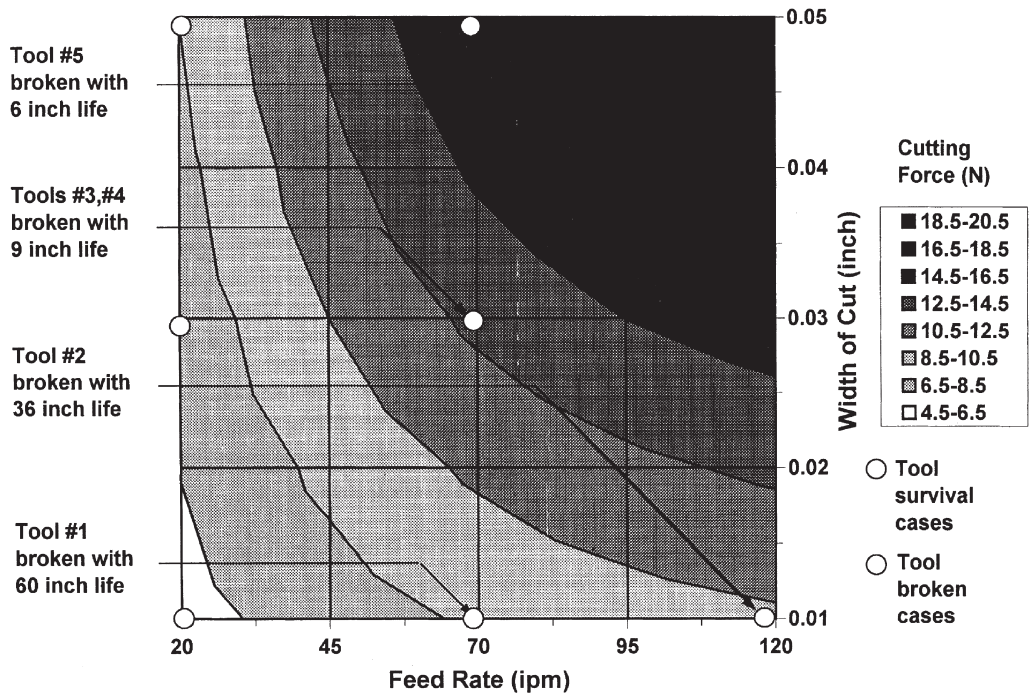

Fig. 5. Experimental feed direction maximum cutting force chart of micro-end-milling operations.

characteristic parameters of the cutting forces directly without using numerical simulators. The model can be simplified for MEMO without run-out and CEMO.

The accuracy of the proposed approach was tested on the experimental data and very good agreement was observed between the theoretical and experimental results. The average error of the model was around 21% when the maximum cutting force was estimated by using the cutting force coefficient obtained in the experiments.

The compact expressions of the proposed approach are very fast and efficient to calculate the characteristics of the cutting forces compared to the numerical approaches. It is feasible to calculate the characteristics of cutting forces in thousands of different cutting conditions to find the optimal ones or to display the results with practical charts. In addition, the compact expressions can be used with optimization algorithms to estimate the tool run-out, machining parameters, surface quality, and tool conditions from the experimental cutting force data.

Computer simulations indicated that tool run-out affects the characteristic of the cutting forces. To minimize the force fluctuations, either the collet-type tool holders should be used or the tool cutting edges should be carefully aligned with the setscrew. The setscrew should be installed with a 90° angle to the cutting edges of two-flute micro-end-mills. The angle with any two adjoining cutting edges should be 45° for four-flute micro-end-mills.

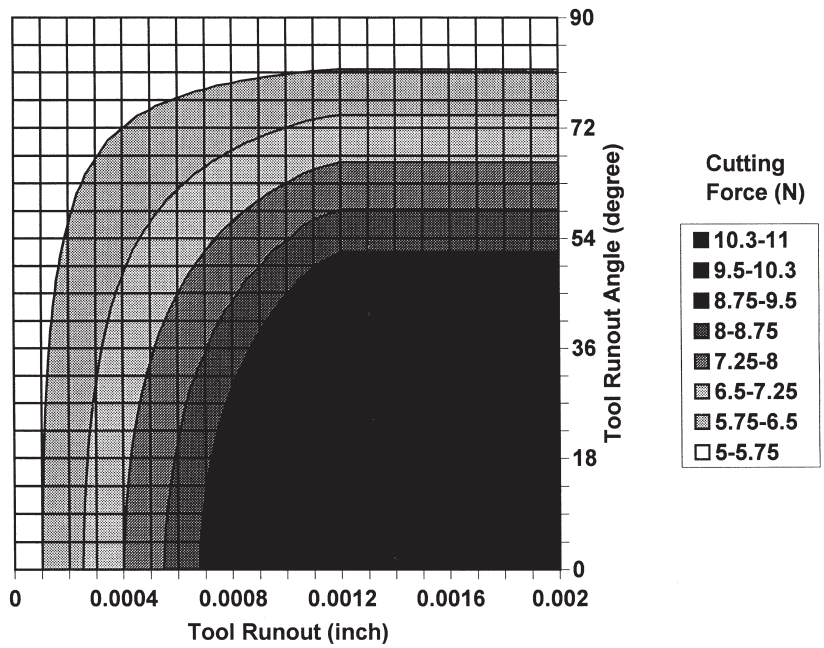

Fig. 6. Simulated normal direction maximum cutting force with tool run-out in 2-D view.

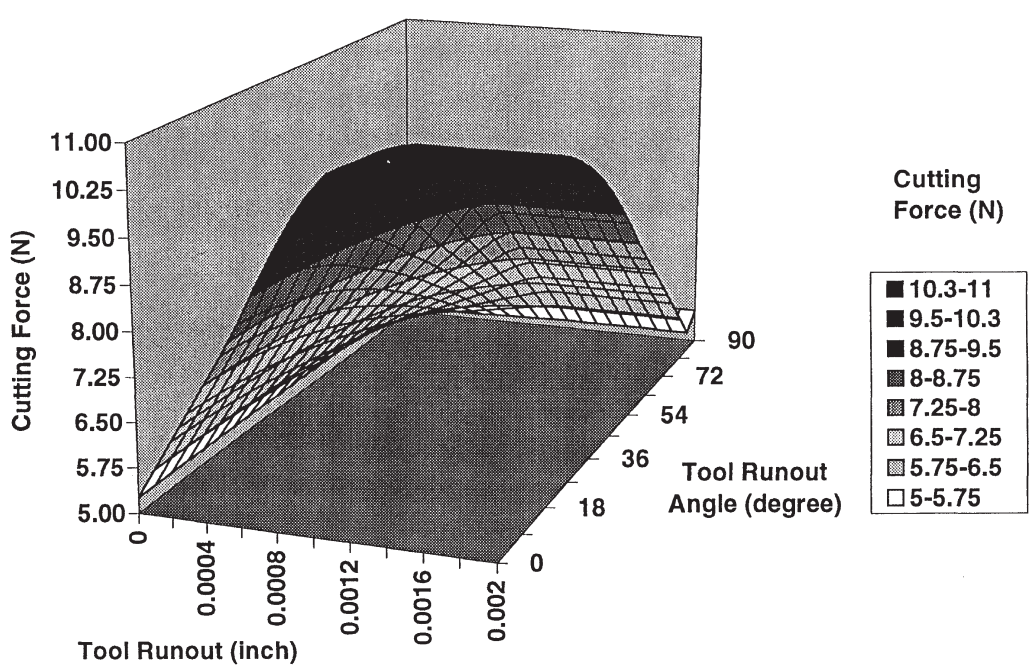

Fig. 7. Simulated normal direction maximum cutting force with tool run-out in 3-D view.

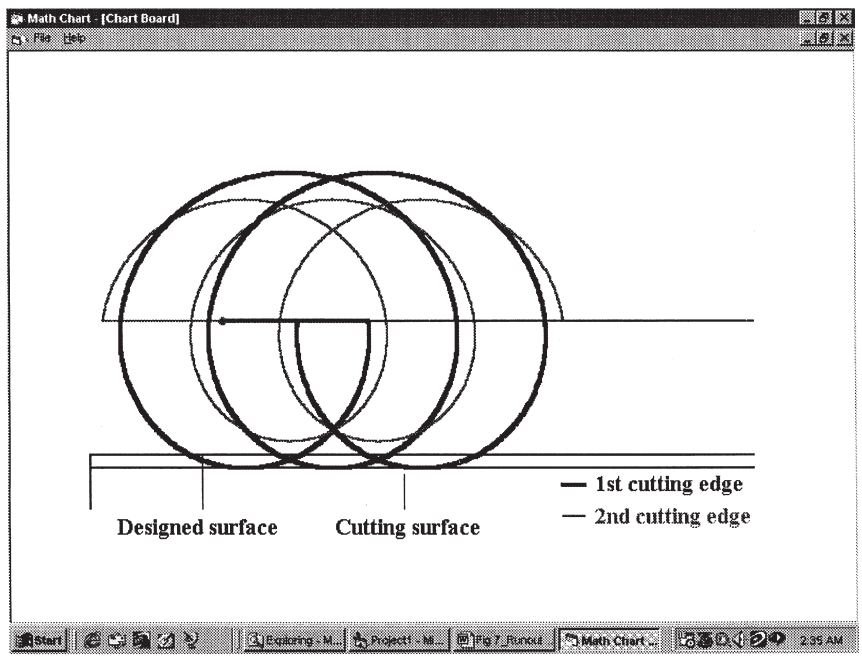

Fig. 8. Trajectory of the two-flute tool tip of micro-end-milling operations with a 0° tool run-out angle.

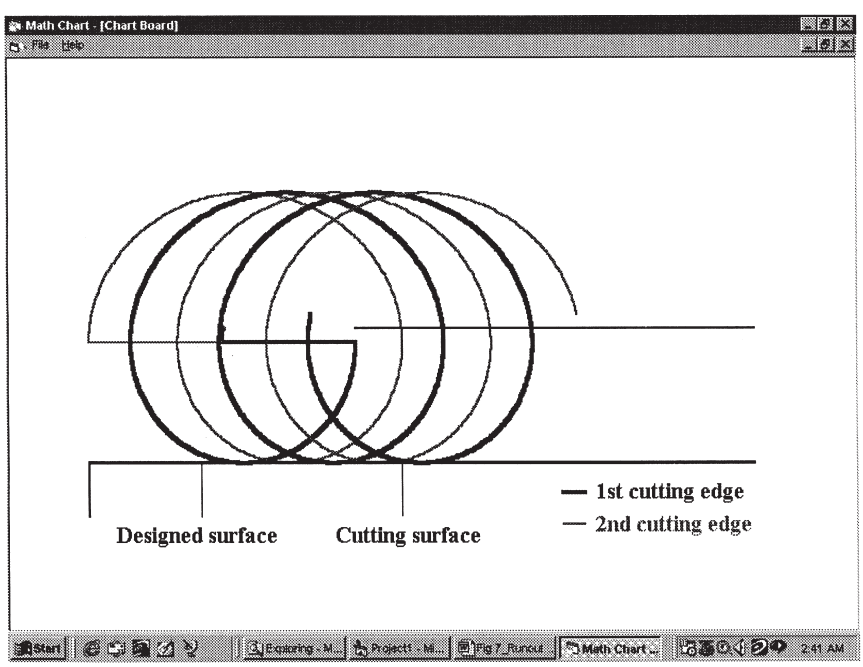

Fig. 9. Trajectory of the two-flute tool tip of micro-end-milling operations with a 90° tool run-out angle.

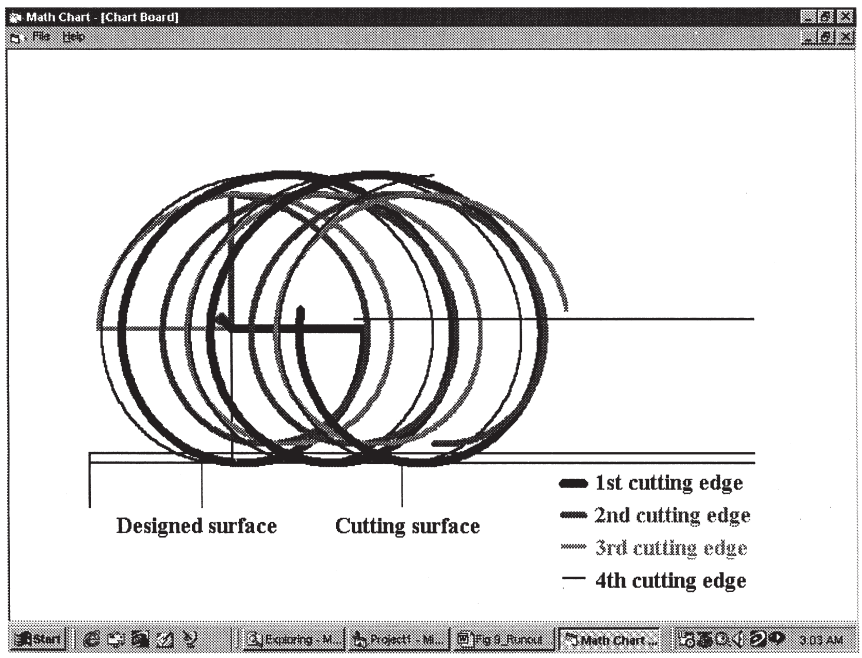

Fig. 10. Trajectory of the four-flute tool tip of micro-end-milling operations with a 45° tool run-out angle.

References

[1] W.Y. Bao, I.N. Tansel, Modeling micro-end-milling operations. Part I: analytical cutting force model, International Journal of Machine Tools and Manufacturing 40 (15) (2000) 2155–2173.
[2] J. Tlusty, P. Macneil, Dynamics of cutting forces in end milling, Annals of the CIRP 24 (1) (1975) 21–25.
[3] F. Gu, S.G. Kapoor, R.E. DeVor, An approach to on-line cutter run-out estimation in face milling, Transactions of the North American Manufacturing Research Institution of SME, pp. 240-247, May 1991.
[4] J.J. Junz Wang, S.Y. Liang, W.J. Book, Convolution analysis of milling force pulsation, Journal of Engineering for Industry 116 (1994) 17–25.
[5] J.W. Sutherland, R.E. DeVor, An improved method for cutting force and surface error prediction in flexible end milling systems, Journal of Engineering for Industry 108 (1986) 269–279.
[6] E.J.A. Armarego, N.P. Deshpande, Computerized end-milling force predictions with cutting models allowing for eccentricity and cutter deflection, Annals CIRP 19 (1) (1991) 25–29.
[7] W.A. Kline, R.E. DeVor, The effect of cutter run-out on cutting geometry and forces in end milling, Int. Jour. of Mach. Tool Des. and Res. 23 (1983) 123–148.
[8] J. Tlusty, F. Ismail, Special aspects of chatter in milling, Trans. of ASME, Journal of Eng. for Ind. 105 (1983) 24–32.
[9] F. Ismail, A. Bastami, Improving stability of slender end mills against chatter, Trans. of ASME, Jour. of Eng. for Ind. 108 (1986) 264–268.
[10] I.N. Tansel, C. McLaughlin, Detection of tool breakage in milling operations: Part 2 — The neural network approach, International Journal of Machine Tools and Manufacturing 33 (4) (1993) 545–558.
[11] I.N. Tansel, W.Y. Bao, T.T. Arkan, B. Shisler, M. McCool, D. Smith, Neural network based cutting force estimators for micro-end-milling operations, smart engineering system: Neural networks, fuzzy logic, data mining, and evolutionary programming, in: InIntelligent Engineering Systems Through Artificial Neural Networks, vol. 7, ASME Press, 1997, pp. 885–890.